Journal of Polymer Research (2020) 27: 207
https://doi.org/10.1007/s10965-020-02142-0

ORIGINAL PAPER

Enhancing proton conductivity of sodium alginate doped with glycolic acid in bio-based polymer electrolytes system

A.F. Fuzlin[1] · M.A. Saadiah[1,2] · Y. Yao[3] · Y. Nagao[3] · A.S. Samsudin[1]

Received: 31 August 2019 / Accepted: 29 April 2020 / Published online: 11 July 2020

Abstract

The investigation on bio-based polymer electrolytes (BBPEs) system based on alginate doped with a various composition of glycolic acid (GA) were carried out and prepared using solution casting technique. The BBPEs complexes were characterized by using fourier transform infrared (FTIR) spectroscopy, X-ray diffraction (XRD), thermal gravimetric analysis (TGA), differential scanning calorimetry (DSC) and electrical impedance spectroscopy (EIS). The complexation was observed to have taken place between alginate and GA with apparent changes of the peak wavenumber, specifically at the $–COO^-$ of alginate functional group. Moreover, from the impedance analysis, it is evident that the sample which contains 20 wt. % of GA possessed the optimum ionic conductivity of 5.32×10^{-5} S cm^{-1} at room temperature with the lowest activation energy. The ionic conductivity increased by incorporating GA was demonstrated via the enhancement of their thermal stability as well as amorphousness. The findings of the present investigation suggest that alginate polymer has the potential to be applied as an electrolyte system for electrochemical devices applications.

Keywords Amorphous materials · Thermal stability · Ionic conductivity · Proton-conducting

Introduction

In recent years, the global demand for energy storage devices have increased significantly primarily due to the rapid increase in portable power-consuming devices, for instance, cellular phones, laptops, and computers, amongst others. Therefore, in order to meet the aforesaid demand, polymer electrolytes (PEs) has shown appreciable traits as an alternative candidate owing to its high flexibility, lightweight nature, as well as, exceptional energy and power density storage. PEs have drawn considerable interest from the research community due to its conductive properties in applications such as solid-state battery [1], solar cell [2], electrochromic devices [3], electrical double-layer capacitor (EDLC) [4] and fuel cell [5]. It is also worth to note that, a dramatic increase in the usage of renewable and biodegradable resources has been demonstrated in the past couple of decades, mainly to cater for a sustainable future. Such resources have and are still being extensively investigated to replace synthetic polymers that are detrimental to the environment.

Therefore, to mitigate this issue, bio-based polymers have been introduced in PEs development, which evidently has been reported to have more superior properties as compared to the conventional synthetic polymer [6]. Amongst its desirable traits are biodegradable, non-toxic, low-cost, abundant and eco-friendly [7]. A plethora of bio-based polymer electrolytes have been discovered, for instance, carboxyl methylcellulose (CMC) [8], chitosan [9], starch [10], cornstarch [11], and carrageenan [12]. These bio-polymers have been reported to provide a favorable ionic conductivity (~10^{-6} to 10^{-4} S cm^{-1} at ambient temperature). Alginate has exhibited a plausible candidate as the backbone polymer matrix in a bio-based polymer electrolytes (BBPEs) systemYang et al. [13]. It was reported to have good conduction and mechanical stability when added with appropriate ionic dopants. Alginate is anionic polysaccharides, which consists of both homopolymeric block (M- and G-) and heteropolymeric block (MG-)

✉ A.S. Samsudin
ahmadsalihin@ump.edu.my

[1] Ionic Materials Team, Faculty of Industrial Sciences and Technology, Universiti Malaysia Pahang, 26300 Pahang, Malaysia

[2] Department of Chemistry, Centre for Foundation Studies, International Islamic University Malaysia, 26300 Gambang, Pahang, Malaysia

[3] School of Materials Science, Japan Advanced Institute of Science and Technology, 1-1 Asahidai, Nomi, Ishikawa 923-1292, Japan

[14, 15]. Alginate is also known as alginic acid, where linear copolymer of uronic acid β-(1–4)-D-mannuronic (M), and α-L-gluronic (G) are residue [16]. Due to their exceptional adhesive properties and non-toxicity, it has been used in a variety of industries, for example, food, pharmaceutical, packaging, and textile industries [17]. Besides, alginate has recently been used in the application of edible films to avoid the usage of conventional packaging plastics, which advertently non-environmental friendly [18].

The concept of dissolving inorganic salts in functional (polar) biopolymer and experimentally creating ion-conducting electrolytes is known as bio-based polymer electrolytes (BBPEs). The interaction between polymer host and doping salt is crucial in determining the ionic conductivity achieved, chemical stability as well as the mechanical strength of the mixture. There are some important factors that may have affect the polymer-ion interactions, such as; (i) molecular weight, (ii) compositions and distance between functional groups, (iii) nature of the functional groups attached to the polymer backbone, (iv) degree of branching, (v) charge of cation, and (vi) counter ions [19]. The ionic conductivity of BBPEs is attributed to the low lattice energy of the complexing salt; thus, increasing the stability of the polymer matrix in BBPEs [20]. Many works have been reported on the various ionic dopant in BBPEs including ammonium salt (ammonium bromide (NH_4Br) [21] and ammonium iodide (NH_4I) [22]), lithium salt (lithium nitrate ($LiNO_3$) [23] and lithium chloride (LiCl) [24]) and acidic salt (phosphoric acid (H_3PO_4) [25] and oxalic acid ($C_2H_2O_4$) [26]).

In the present work, the investigation on proton conducting materials based bio-based polymer electrolytes (BBPEs) system has been carried out by using alginate as biopolymer host and doped with glycolic acid (GA). Glycolic acid (GA) is the simplest form of carboxylic acid, which contains highly polar organic groups and two important H-bonding sites; (i) carboxyl C=O and (ii) hydroxyl O-H. This would promote the formation of amorphous complexes through intra- and inter- molecular attraction with the polymer chain [27]. GA is considered as an ionic dopant that can provide a conduction pathway for the conducting species to migrate through the polymer matrix under the influenced of an electric field [28]. The structural and ionic conduction properties of BBPEs were characterized by using Fourier Transform Infrared (FTIR) spectroscopy, X-Ray Diffraction (XRD), Thermal Gravimetric Analysis (TGA), Differential Scanning Calorimetry (DSC) and Electrical Impedance Spectroscopy (EIS). Furthermore, the ionic transport properties were investigated via FTIR-deconvolution technique for analyzing the details on the ionic conduction behavior of alginate-GA based BBPEs system.

Experimental

Preparation of bio-based polymer electrolytes

In this work, bio-based polymer electrolytes (BBPEs) sample-based alginate (Sigma Aldrich with M.W.: ~120,000) and glycolic acid, GA (Merck Co. with M.W.: 76.05 g/mol has been prepared by using solution casting technique. For the preparation, alginate was dissolved in distilled water, and then, different compositions (in wt.%) of GA were added into the alginate solution. The mixture was stirred until a homogenous solution was obtained and poured into a petri dish. The solution was left in the oven at 60 °C for overnight until the film was formed. The film was further drying in desiccators filled with silica gel to prevent any solvent trapped in BBPEs system. The summarized of sample preparation, physical appearance and designation of the sample are illustrated in Fig. 1.

Characterization of alginate-GA BBPEs system

Fourier transform infrared spectroscopy (FTIR)

Fourier Transform Infrared (FTIR) spectroscopy measurement was carried out to identify the complexation between alginate and GA in the BBPEs system. The infra-red spectra were obtained using Perkin Elmer Spectrum 100 with an attenuated total reflection (ATR) accessory with a germanium (Ge) crystal. The infra-red light was passed through the sample with the frequencies in the range between 700 cm^{-1} until 4000 cm^{-1} with spectra resolution of 2 cm^{-1}.

Thermal gravimetric analysis (TGA)

TGA was carried out by using TG-DTA2010SA (NETZSCH Japan K.K., Japan). The measurements were recorded in a nitrogen gas atmosphere at a flow rate of 100 ml min^{-1}. The BBPEs system was weighing with ~2 mg and placed into the aluminum pan. The samples were tested at different temperature ranging from 30 to 550 °C at a heating rate of 10 °C min^{-1}.

Differential scanning Calorimetry (DSC)

DSC was carried out by using NETZSCH DSC 214 Polyma model. The measurements were recorded in a nitrogen gas atmosphere at a flow rate of 62 ml min^{-1}. The BBPEs system was weighing with ~2 mg and placed into the silica crucible. The samples were tested at different temperature from 30 to 200 °C at a heating rate of 30 °C min^{-1}.

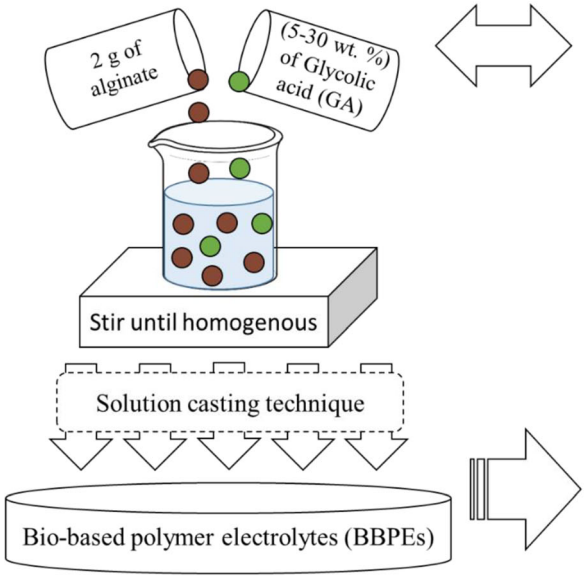

Designation	Weight percentage of GA (wt. %)
ALGA-0	PURE ALGINATE
ALGA-1	5
ALGA-2	10
ALGA-3	15
ALGA-4	20
ALGA-5	25
ALGA-6	30

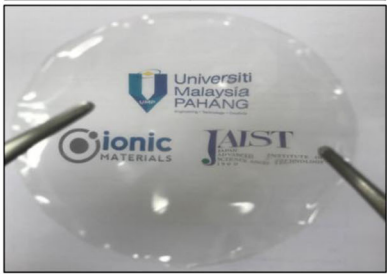

Fig. 1 Samples preparation, designation of sample, and physical appearance of alginate-GA BBPEs system

X-ray diffraction (XRD)

X-ray diffraction (XRD) is the technique to determine the phase of crystalline and amorphous of polymer-salt complexes. X-ray diffraction depends on constructive interference of monochromatic x-rays and a sample by using Bragg's law. MiniFlex II from Rigaku had performed to run out the nature of the present sample (amorphous/crystal) at different angles of 2θ between 5° and 80° with 1.5406 Å wavelength generated by a $C_u K_d$ source. The XRD deconvolution analysis was carried out using OriginPro 9.0 software. Based on the assumption of Gaussian's peak function, the crystalline and amorphous peaks were deconvoluted to ensure that all peaks fit with the original spectra. The percentage crystallinity of the BBPEs system is calculated by using the following equation:-

$$X_c = \frac{A_c}{A_T} \times 100\% \quad (1)$$

Where A_c is the area covered under crystalline region, A_T is the total area covered under the whole diffractogram (total of area of crystalline and amorphous region), and X_c is the degree of crystallinity in percentage.

Electrical impedance spectroscopy (EIS)

Electrical Impedance Spectroscopy (EIS) is used to evaluate the ionic conduction properties of BBPEs system. The present samples were cut into a suitable size and sandwiched between

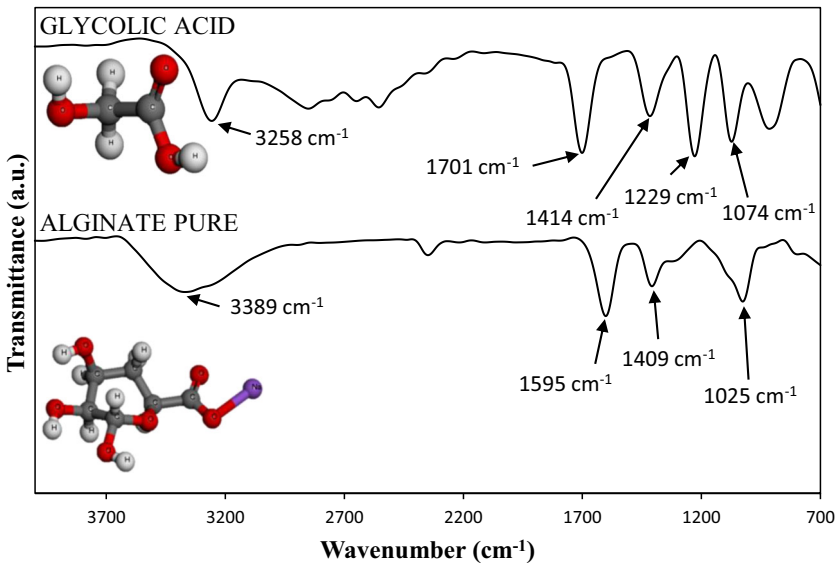

Fig. 2 FTIR spectra of pure alginate and pure glycolic acid. Inset shows the optimized structure of alginate polymer and glycolic acid using Material Studio 2017

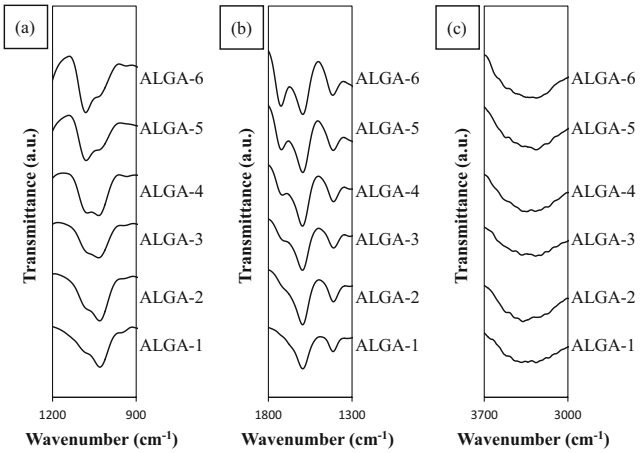

Fig. 3 FTIR spectra of alginate-GA BBPEs system between range (**a**) 900 cm^{-1} to 1200 cm^{-1} (**b**) 1300 cm^{-1} to 1800 cm^{-1} (**c**) 3000 cm^{-1} to 3700 cm^{-1}

the stainless steel (SS) electrodes and left into the oven in order to control the humidity of the environment [29]. The prepared samples were measured using a HIOKI 3532–50 LCR Hi-Tester with frequencies ranging from 50 Hz to 1 MHz. The ionic conductivity of sample-based alginate-GA BBPEs system was calculated using equation:

$$\sigma = \frac{t}{R_b A} \tag{2}$$

Where t (cm) is the thickness of sample, A (cm^2) is the electrode-electrolyte contact area and R_b (Ω) is bulk resistance of BBPEs system which can be obtained from the Cole-Cole plot of EIS.

Transport parameter study

The transport properties of the thin film based alginate-GA BBPEs system were determined using FTIR deconvolution. Deconvolution was analyzed using Gaussian-Lorentz function, which was adapted to the OriginPro 9.0 software. In this method, the FTIR peaks due to complexation of alginate and GA were carefully selected based on dominant ionic movement. Besides, the sum of all the intensity of the deconvoluted peaks was ensured to fit the original spectrum. The absorbance peaks were fitted to a straight baseline and the area under the peaks was determined [30]. The free ions percentage (%) were calculated using the equation [31, 32]:-

$$Percentage\ of\ free\ ions\ (\%) = \frac{A_f}{A_f + A_c} \times 100\% \tag{3}$$

Where A_f is an area under the peak representing the free ions region, A_c is the total area under the peak representing the contact ions. The transports parameter such as number density (η), mobility (μ) and diffusion coefficient (D) of the ions were calculated following this equation [22, 33]:-

$$\eta = \frac{MN_A}{V_{Total}} \times free\ ions\ (\%) \tag{4}$$

where:

$$V_{Total} = \left[\frac{weight}{density}(alginate)\right] + \left[\frac{weight}{density}(GA)\right] \tag{5}$$

$$\mu = \frac{\sigma}{\eta e} \tag{6}$$

$$D = \frac{KT\mu}{e} \tag{7}$$

Where M is number of moles of GA used, N_A is the Avogadro's constant (6.02×10^{23} mol^{-1}), V_{total} is total volume of BBPEs system, k is the Boltzmann constant (1.38×10^{-23} J K^{-1}), T is the absolute temperature in Kelvin and e is the electric charge (1.602×10^{-19} C).

Result and discussion

FTIR analysis

In the present work, the structural arrangement of alginate and glycolic acid were studied using density functional theory. By using DMol3 modules of Material Studio 2017 software, the

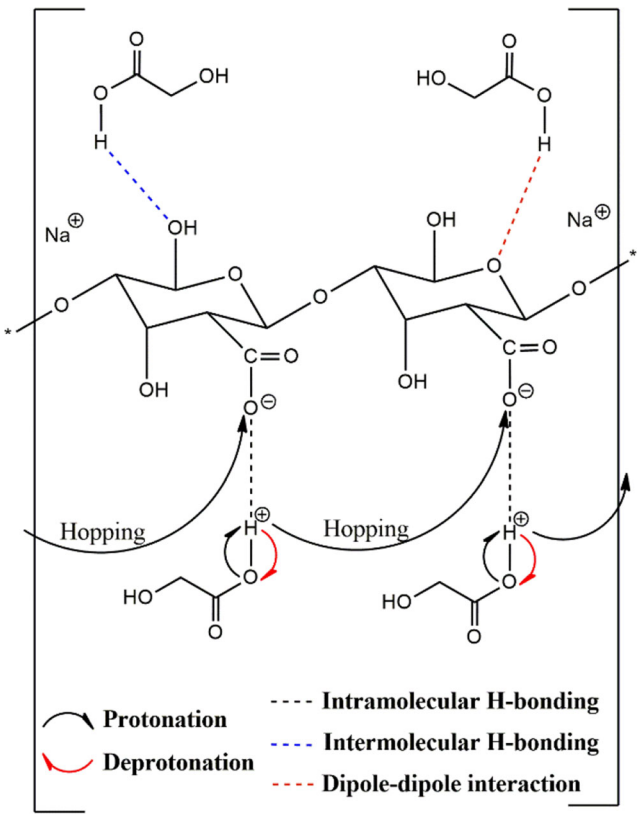

Scheme 1 Schematic diagram of alginate having interacted with GA.

Table 1 Summary of peak changes in wavenumber for alginate-GA in BBPEs system

Wavenumber (cm^{-1})								Assignments (functional group)
GA	ALGA-0	ALGA-1	ALGA-2	ALGA-3	ALGA-4	ALGA-5	ALGA-6	
–	1025	1030	1031	1035	1035	1080	1081	C–O–C stretching
1074	–	–	–	–	–	–	–	C-O stretching
1229	–	–	–	–	–	–	–	O-H bending
–	1409	1415	1411	1417	1413	1417	1417	($–COO^-$) symmetric stretching
1414	–	–	–	–	–	–	–	$–COO^-$ stretching
–	1595	1595	1596	1596	1597	1595	1594	($–COO^-$) asymmetric stretching
1701	–	–	1708	1715	1721	1727	1730	C=O stretching
3528	3389	3350	3342	3328	3335	3305	3298	O-H stretching

alginate model and glycolic acid was optimized through geometry optimization and energy minimization. The FTIR spectrum of alginate and GA were presented in Fig. 2, and the inset figure depicts the optimized structure of alginate monomer and glycolic acid (GA). The FTIR spectra confirmed the alginate structure as all characteristic peaks were observed at 1025 cm^{-1}, 1409 cm^{-1}, 1595 cm^{-1}, 2325 cm^{-1} and 3389 cm^{-1} which are attributed to glycoside bond (C–O–C) [34], symmetric stretching of $–COO^-$ [35], antisymmetric stretching of $–COO^-$ [36], and stretching –OH group [37] respectively. From the spectra of pure GA, strong absorption peaks at 1074 cm^{-1}, 1229 cm^{-1}, 1414 cm^{-1}, 1701 cm^{-1}, and 3258 cm^{-1} that correspond to the stretching of C-O [38], bending O-H [39], stretching of the $–COO^-$ [40], stretching of C=O [41], and stretching O-H group [42], respectively were observed.

Figure 3 shows the highlighted FTIR spectrum for the bio-based polymer electrolytes (BBPEs) system, which represents the complexes of alginate-GA. The complexation between host polymer and ionic dopant can be identified through the changes of the wavenumber or the peak intensity in the FTIR spectrum. In this present system, it is expected the group of interest that would lead to the complexation between alginate and GA is at the polar groups of C–O–C, $–COO^-$ and –OH in the biopolymer matrix due to the presence of lone pair electrons of the coordinating site (O) that attract the cation from the salt molecule [43].

Figure 3 (a) shown the peak at 1025 cm^{-1} for ALGA-1 which corresponds to the C–O–C stretching vibration [44] has shifted to 1030 cm^{-1} (higher wavenumber) which is believed due to the coordination of proton (H^+) to the glycoside group (C–O–C) of alginate [45]. This glycoside band of polysaccharide alginate molecule was shown to further shifted until 1081 cm^{-1} for ALGA-6, which indicates that the complexation at the C–O–C via weak van der Waals attraction of dipole-dipole forces upon the inclusion of acidic salt become apparent.

Another significant peak was observed between 1300 to 1700 cm^{-1} belonged to symmetrical and asymmetrical carboxylate, $–COO^-$ as shown in Fig. 3 (b). This region was expected to exhibit strong affinity towards the GA due to highly nucleophilicity of the carboxylate ion [46]. The increasing salt composition leads to change in wavenumber for ALGA-1 until ALGA-6. In the present work, H^+ cation

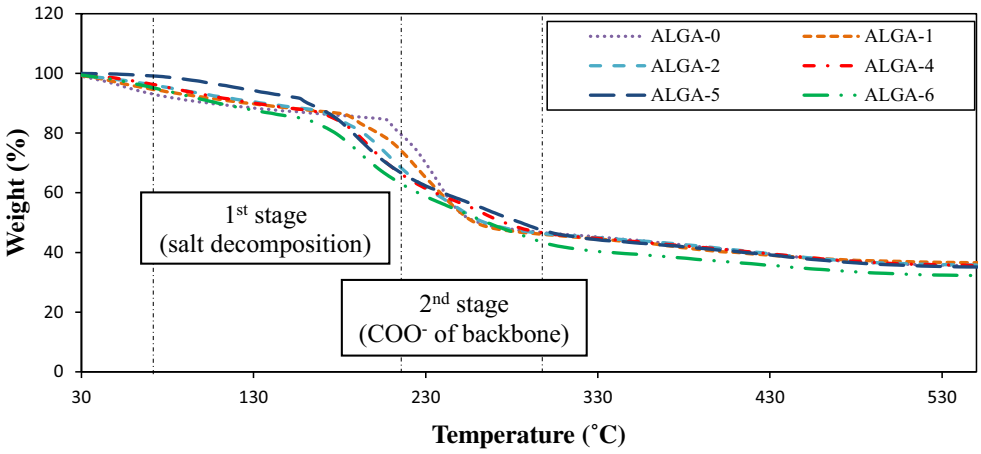

Fig. 4 Thermal spectra of alginate-GA in BBPEs system

Table 2 Thermal properties of alginate-GA in BBPEs system

Sample	Weight loss (Δ %)		Maximum temperature (°C)	
	1st stage	2nd stage	1st stage	2nd stage
ALGA-0	15.80	32.82	207.81	255.14
ALGA-1	13.70	36.39	183.34	259.43
ALGA-2	13.00	37.38	170.92	266.79
ALGA-4	13.35	38.92	169.84	287.82
ALGA-5	8.27	43.69	156.23	294.58
ALGA-6	15.97	40.57	163.56	297.20

from GA acts as a function of an electrophile positive ion. It could interact with the oxygen atom of carboxylate anion group present in alginate biopolymer via electrostatic attraction to form [H^+—$^-$OOC], thus prominent to the increment of intensity peak of BBPEs system [47, 48]. Notably, due to this strong attraction, the wavenumber has shifted from 1409 to 1413 cm^{-1} and 1595 to 1597 cm^{-1} for symmetry –COO^- and asymmetry –COO^- respectively [49]. This interaction was expected due to the coordination interaction of (–COO^-) moiety in alginate with H^+ ion of [-COOH] substructure in GA which reflects the protonation between the cation (H^+) and the carboxylate group of alginate and triggers the ion hopping phenomenon called Grotthuss mechanism [50]. The H^+ ion hopping from hydroxyl moiety to the carboxylate group of each monomer of alginate electrolyte and affect the changes in crystallinity phase and ionic conductivity.

Furthermore, upon addition of more GA, (more than 20 wt. %) the peak shifted to 1417 cm^{-1} and 1594 cm^{-1} for symmetry –COO^- and asymmetry –COO^- respectively. Rasali and Samsudin [33] reported that the phenomenon of shifted in wavenumber at –COO^- at BBPEs system might be due to salt aggregation, which may affect the conductivity of the polymer electrolyte. The new peak was observed by the addition of GA as shown in Fig. 3 (b). The peak at ~1710 cm^{-1} belongs to C=O stretching of GA. The same phenomenon was founded in Chai and Isa [51] work, where new appearance peak at ~1710 cm^{-1} belongs to C=O stretching of GA.

The broad band was identified at 3389 cm^{-1} as shown in Fig. 3 (c) is known for the stretching O-H group in alginate monomer. It could be seen that it was shifted towards a lower wavenumber 3350 cm^{-1} when GA was introduced. This finding was found to be similar to Alakanandana et al. [52] where they observed the occurrence of intermolecular hydrogen bonding has occurred between polyvinyl alcohol (PVA) and succinic acid. Overall, the FTIR result has revealed and confirmed various interactions during the complexation between alginate and GA that are favorable in the conductivity

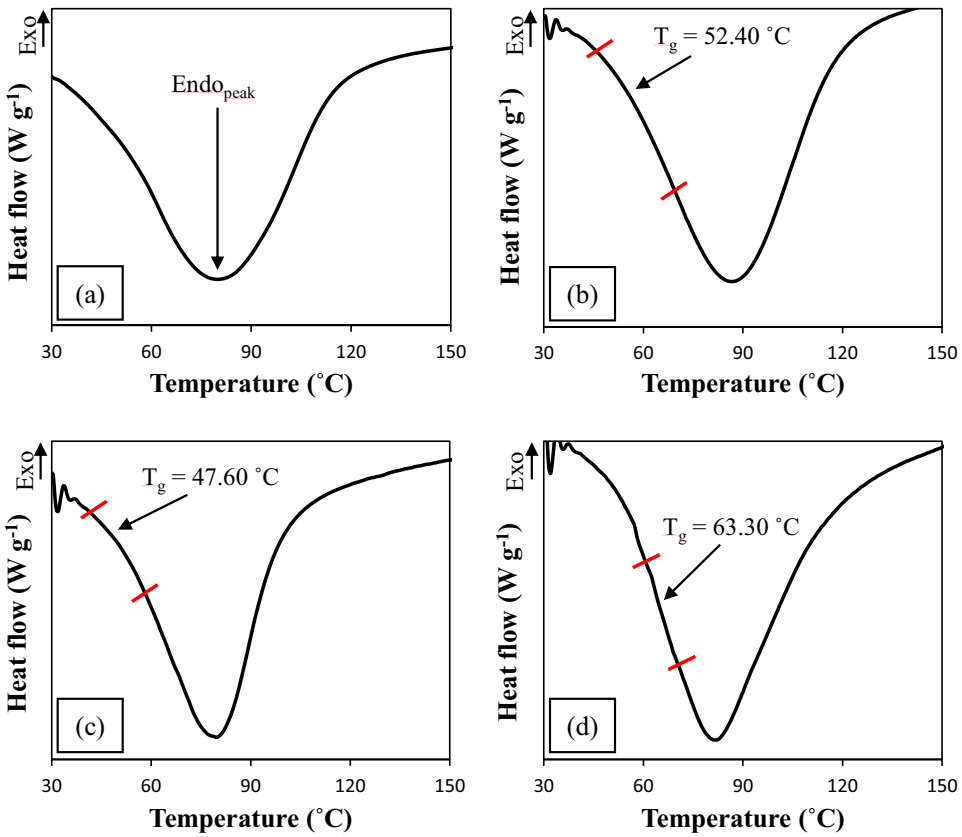

Fig. 5 DSC thermograms for (**a**) ALGA-0 (**b**) ALGA-2 (**c**) ALGA-4 and (**d**) ALGA-6 of BBPEs system

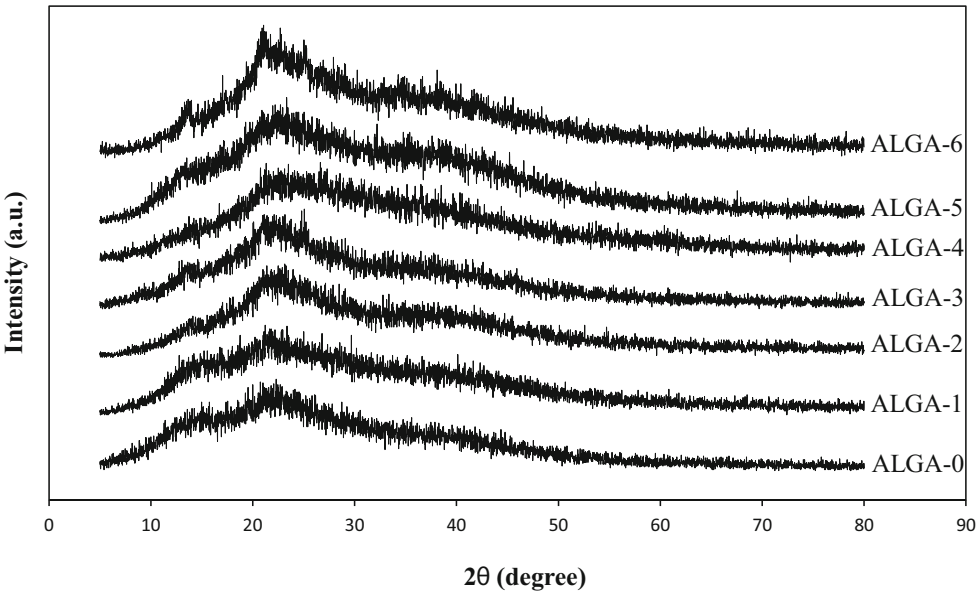

Fig. 6 XRD spectra for alginate-GA BBPEs system at ambient temperature

enhancement. Schematic mechanism of the interaction between H^+ of GA and interaction site of alginate is expected to occur based on Scheme 1, and all the functional groups change in wavenumber is presented in Table 1.

Thermal behavior

Thermogravimetric analyses (TGA) was carried out to figure it out the effect of the GA on the thermal stability in BBPEs. TGA curves of alginate BBPEs system doped with various composition of glycolic acid was shown in Fig. 4. Two major decomposition stages were observed in the temperature range of 30 °C until 550 °C and tabulated in Table 2.

The initial weight loss for BBPEs system at 30 °C to 70 °C is attributable to the loss of the moisture where the alginate biopolymer tends to absorb the water and solvent for entire samples [53, 54]. The first decomposition was observed at an intermediate temperature range from 70 °C to 200 °C and involved small weight loss (10–15%) due to the decomposition of glycolic acid. It can be seen that decomposed temperature, T_d for alginate doped with GA was relatively lower than pure alginate. This finding was supported by Qu et al. [55], where the addition of GA, resulting in the lower T_d value, which is attributed to the low thermal stability of GA side chains. For the second stage of decomposition, un-doped sample (ALGA-0) has lost approximately 32.82% of its weight, at temperature ~ 250 °C. The weight loss is due to the loss of $-COO^-$ from the polysaccharide of alginate matrix [56]. Though, the T_d was observed to increase linearly upon the addition of GA may be attributed to the complexation that has been taken place, which required a higher temperature for the disruption of H-bonding [57, 58]. A similar finding has been reported by Fadzallah et al. [26] for the system based on chitosan complexed with oxalic acid where the addition of acid salt enhances the thermal stability of BBPEs system. Therefore, it shows that the increment composition of GA in BBPEs system has a good thermal stability, which is beneficial in the fabrication of the device application.

It can be observed that prolong heating beyond 550 °C of decomposition temperature BBPEs system resulting in the carbonization and ash formation [59, 60]. This result reveals that the alginate can be used as a host polymer at various temperature, which is suitable for BBPEs system [61].

DSC analysis

Differential scanning calorimetry (DSC) was used to characterize the thermal behavior of materials, which can further confirm the miscibility of alginate and GA by measuring the changes in the heat capacity as the polymer matrix goes from the glass state to rubber state as known as T_g [62, 63]. Figure 5 displayed DSC thermograms obtained for BBPEs system and the glass transition temperatures (T_g) are depicted by arrows as shown in the figure. Based on Fig. 5(a), The T_g value for ALGA-0 was not detected at this range of temperature study. However, endothermic peaks were found at ~80 °C indicates further removal process of loosely bound water present in sodium alginate. As reported by Ghosal et al. [64] and Rezvanian et al. [65], the endothermic peak observed at temperatures 80.02 °C attributed to the evaporation of adsorbed moisture and dehydration of the cross-linked polymer matrix.

In BBPEs system, The T_g started to appear when glycolic acid (GA) added to alginate. From Fig. 5(b), the addition of 10 wt. % GA started to show the T_g value due to the formation of coordination between the polymer chain segments and ions formation from ionic dopant which increases the energy

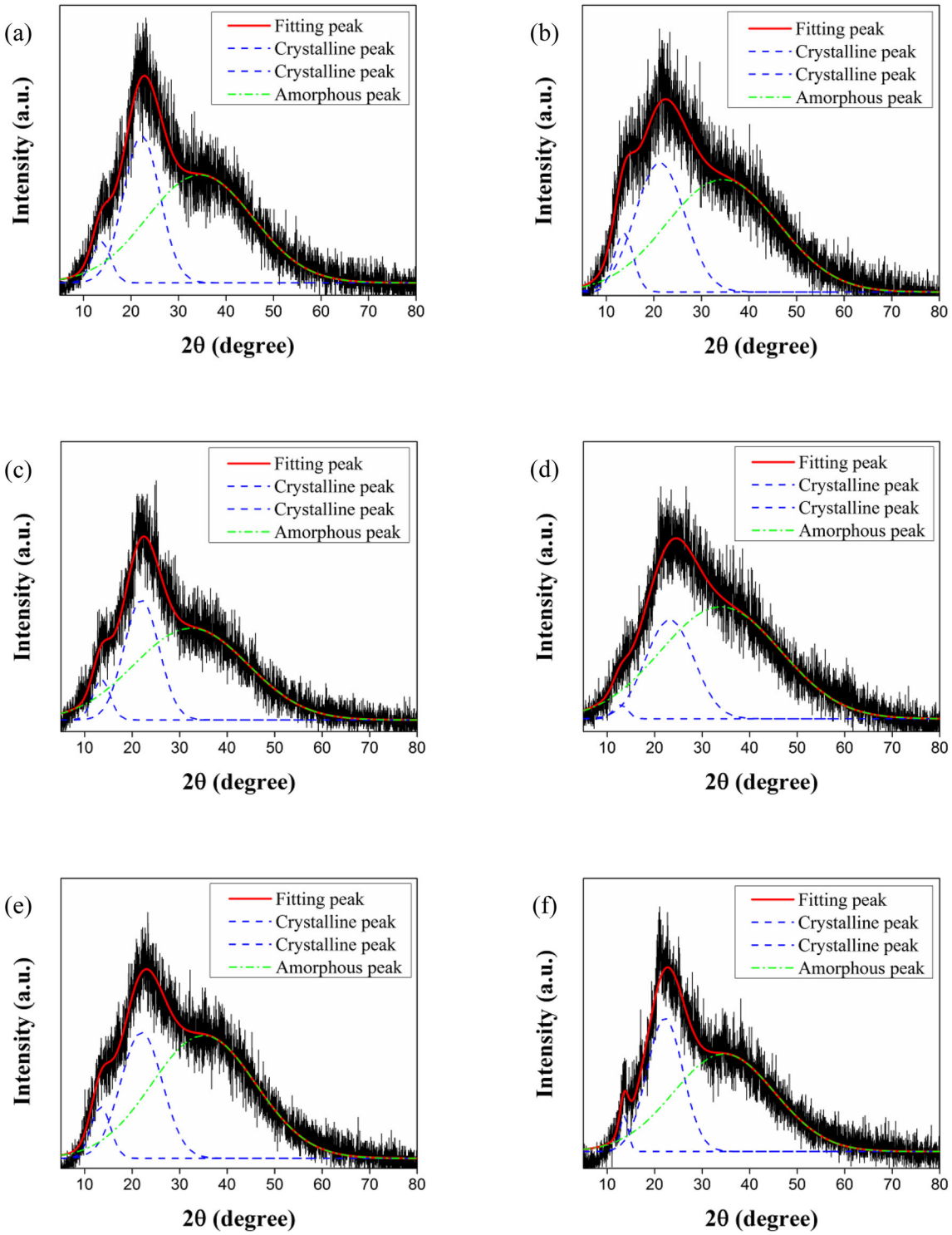

Fig. 7 XRD deconvolution patterns for (**a**) ALGA-1 (**b**) ALGA-2 (**c**) ALGA-3 (**d**) ALGA-4 (**e**) ALGA-5 and (**f**) ALGA-6 of BBPEs system

barrier to the segmental motion of the polymer chains; thus, the stiffening of the polymer chains may occur [66]. The lowest T_g value of ALGA-4 ($T_g = 47.60$ °C) indicates an increase in the flexibility of alginate chains; hence, the ALGA-4 was expected to exhibit the highest ionic conductivity value [67]. Further increase in the composition of GA leads to the increment of T_g value ($T_g = 63.30$ °C) for sample ALGA-6. It can be attributed to the formation of ion aggregates in the alginate polymer matrix, which reduced the flexibility of the polymer chain [68]. A similar trend has been observed by Moniha et al. [69] for the system based on iota carrageenan complexed with ammonium nitrate (NH_4NO_3).

Table 3 Degree crystallinity of alginate-GA in BBPEs system

Sample	Degree of crystallinity, X_c (%)
ALGA-0	45.35
ALGA-1	37.29
ALGA-2	34.98
ALGA-3	31.99
ALGA-4	26.99
ALGA-5	32.82
ALGA-6	34.16

X-ray diffraction analysis

Figure 6 shows typical x-ray diffractogram for alginate-GA BBPEs system. It can be seen that ALGA-0 has a broad amorphous peak occur at the central position with $2\theta = 37.56°$. This indicates that pure alginate has two different regions of amorphous [70]. The crystalline peak at 13.50° and 22.40°of ALGA-0 is observed in the present system which shown the characteristic of alginate and found to be similar to other research works [71, 72].

The XRD pattern of BBPEs system show an increase in broad peak with the addition of 0–20 wt. % GA. The broad peak is a typical characteristic of amorphous material [67]. According to Yusof et al. [73], no crystalline peaks found might be due to complete salt dissociation in the polymer matrix. Therefore, an increase in ionic conductivity of the alginate-GA BBPEs system is expected due to the changes of amorphousness and low glass transition in the samples [74]. Based on Fig. 6, it can be seen that the intensity of the broad peak reduced upon the addition of 20 wt. % GA indicating that complexation occurred significantly between alginate and GA. This might be attributed to the greater ionic diffusivity, where the addition of GA managed to enhance the intramolecular and intermolecular interaction through hydrogen bonding in BBPEs system, and thus exhibiting the amorphous characteristic [75, 76].

It shows that, above the addition of 20 wt. % GA, the intensity XRD pattern start to increase with small crystalline peaks at $2\theta = 24.80°$ was observed. The increment of peak intensity was expected to decrease the number of mobile ions and hence affecting the ionic conductivity of the BBPEs system. According to Shukur et al. [77], the increment of the crystalline peak of BBPEs system will be correlated to the ionic conductivity and could be due to recombination of the ions, where the polymer host was incapable of accommodating the ionic dopant [78].

Figure 7 presents the XRD deconvolution patterns for BBPEs system. The percentage of crystallinity for un-doped alginate is obtained at 45.35% nd when added with 5 wt. % of GA, it demonstrated a decrement to 37.29%. The incorporation of GA into the host biopolymer induces a small increase in the amorphous structure, which attributed to the decrement of percentage crystallinity in BBPEs system. Based on the calculated value in Table 3; ALGA-4 depicts the lowest percentage of crystallinity which is 26.99% and this stimulates the segmental motion of the polymer matrix by reducing the energy barrier; hence, high ionic diffusivity is expected to enhance the ionic conductivity of the BBPEs system [66]. However, the increment percentage of crystallinity was observed for the composition of GA above ALGA-4. This may be due to the recombination of ions, which eventually lead to decrement in ionic conduction [22].

Ionic conductivity analysis

Figure 8 shows the ionic conductivity values of alginate samples containing different amounts of GA at ambient temperature. The increment of ionic conductivity with the

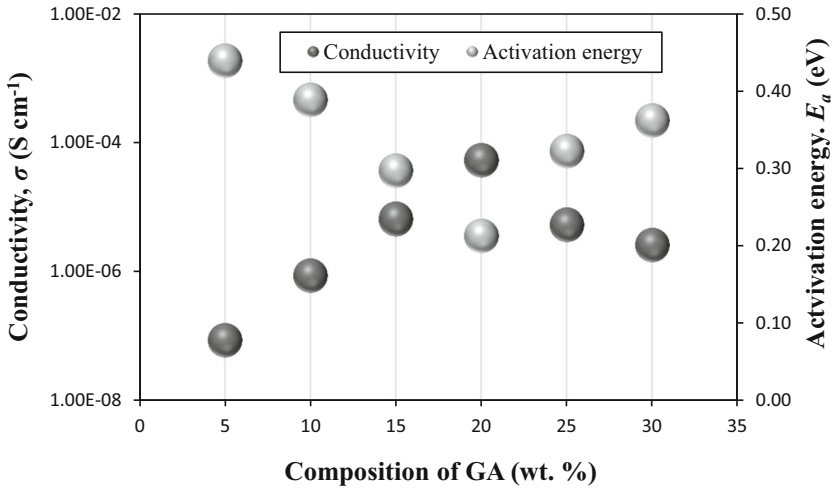

Fig. 8 The conductivity and activation energy of alginate-GA BBPEs system at ambient temperature

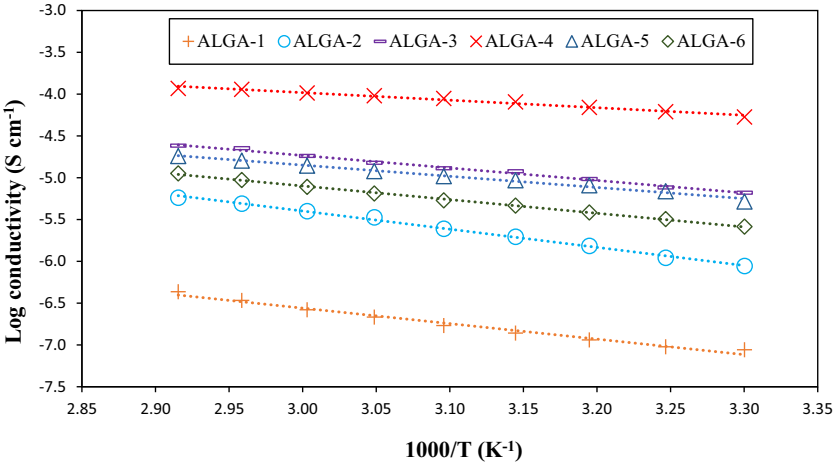

Fig. 9 The conductivity of alginate-GA BBPEs system at different temperature

addition of GA can be related to increment of mobile charge carrier in BBPEs. As discussed earlier in FTIR analysis, the complexation between alginate and GA has shown high dispersion (dissociation of salt) of H^+ and coordinate with the anion group of alginate bio-based polymer; therefore it would affect the increment of the ionic conductivity [79, 80]. Moreover, the amorphous structure and low glass transition temperature, T_g enhanced the migration of H^+ ions (hopping) from GA to the coordination site (oxygen) of alginate host [81]. In the present system, the highest ionic conductivity at room temperature was found at 5.32×10^{-5} S cm^{-1} for the sample containing with 20 wt. % of GA (ALGA-4). The enhancement of ionic conductivity to the optimum value was found to align with the observation from XRD and DSC analysis.

Upon addition of GA beyond sample ALGA-4, the ionic conductivity started to decrease. According to Othman et al. [82], the decrement of ionic conductivity after ALGA-4 because of neutral aggregation of the ions re-associated and also leading to the formation of ion cluster as revealed by structural analysis. The decrement of ionic conductivity also was due to the formation of re-crystallization at polymer matrix, as shown in XRD study. The crystallize region of BBPEs system barricades the movement of ions when the conductivity starts to decrease at higher composition of GA [32].

Figure 9 shows the log conductivity versus 1000/T for different composition at the temperature range from 303 K to 343 K. The increasing of temperature depicts there is no sudden drop in conductivity value, which indicates that BBPEs system is good thermal stability and completely amorphous as observed in XRD and DSC analysis. As the temperature increases, the migration of charge carrier has promoted, which leads to an expansion in the polymer matrix [83, 84]. This expansion in the polymer network provides free volume to promote the motion of charge carriers and increases the conductivity. The temperature-dependent study of the BBPEs system obeys the Arrhenius characteristics, where the regression value, R^2, is in the range of 0.95 to 0.99. [85, 86]. From the temperature-dependent study, activation energy, E_a can be calculated by using the Arrhenius equation.

$$\sigma = \sigma_o \exp\left(-\frac{E_a}{kT}\right) \tag{8}$$

where σ_o is pre-exponential factor, k is Boltzmann's constant and T is the temperature in Kelvin. The E_a values were calculated based on the slope of the temperature dependence plot and depicted in Fig. 8. It is noted that for alginate-GA BBPEs system, the activation energy decreases linearly as the conductivity increase. ALGA-4 showed the lowest value of E_a (0.18 eV) indicates that H^+ from biopolymer matrix need lesser energy to migrates the ions to other coordinating sites thus creating vacancy sites for other H^+ to complete the "hopping mechanism" of BBPEs system [48, 87]. The result indicates that increasing of GA composition not only would lead to enhance the number of carriers, but also reduce the energy barriers of BBPEs system [88].

Transport parameter analysis

In the present work, FTIR deconvolution for various sample of alginate-GA BBPEs system was presented as shown in Fig. 10. Hay and Myneni [41] reported that strong absorption peaks at ~1420 cm^{-1} denote the anion vibration mode of $-COO^-$ from alginate, which proved the IR active in FTIR study. According to Ramlli et al. [40], the area of deconvoluted peak was determined based on significant change of wavenumber which was believed there is occurrence of complexation between the polymer and ionic dopant, and based on that, it leads to the need of separation the free ions and contact ions within the region. Based on Fig. 10, the BBPEs system shows free ions occurred at ~1410 cm^{-1}, while contact ions appeared at ~1400 cm^{-1} and ~ 1430 cm^{-1} [45].

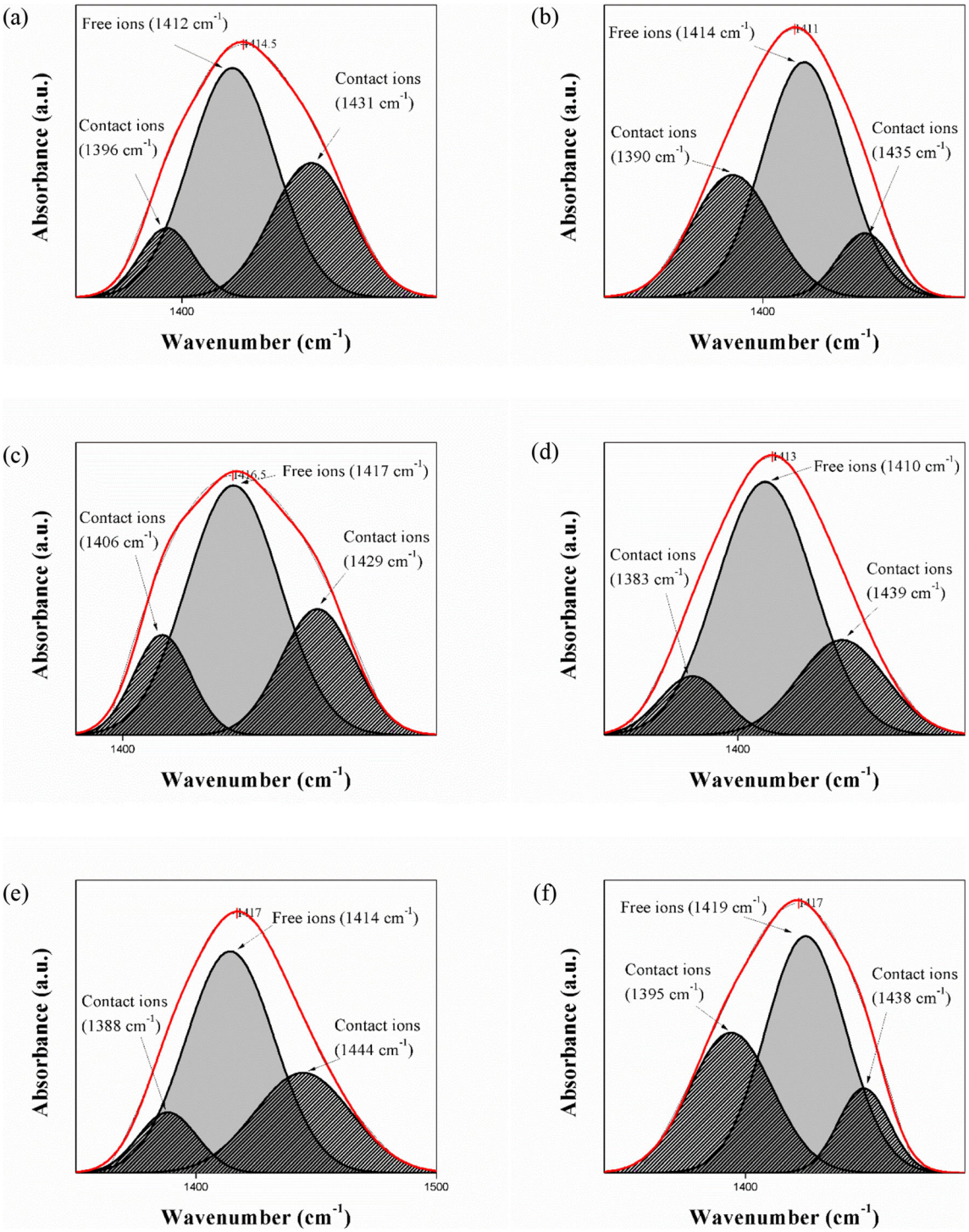

Fig. 10 The deconvolution IR spectrum for samples (**a**) ALGA-1 (**b**) ALGA-2 (**c**) ALGA-3 (**d**) ALGA-4 (**e**) ALGA-5 and (**f**) ALGA-6 of BBPEs system

The free ions and the contact ions were calculated and depicted in Fig. 11.

From Fig. 11, it shows that the addition of GA increases the percentage of free ions until sample ALGA-4. This can be due to the increase ion dissociation of hydrogen ion (H^+), thus resulting in more ion conduction, which eventually increasing the ionic conductivity in BBPEs system [33]. Beyond the 20 wt. % of GA, the percentage of free ions started to decrease linearly due to a large number of ion pairs and ion aggregates which accumulate in alginate bio-based polymer matrix as proven from XRD analysis [89]. Besides, the decrement of ionic conductivity is due to the re-associated of ions which supported the ionic conductivity reductions of alginate-GA BBPEs system [90].

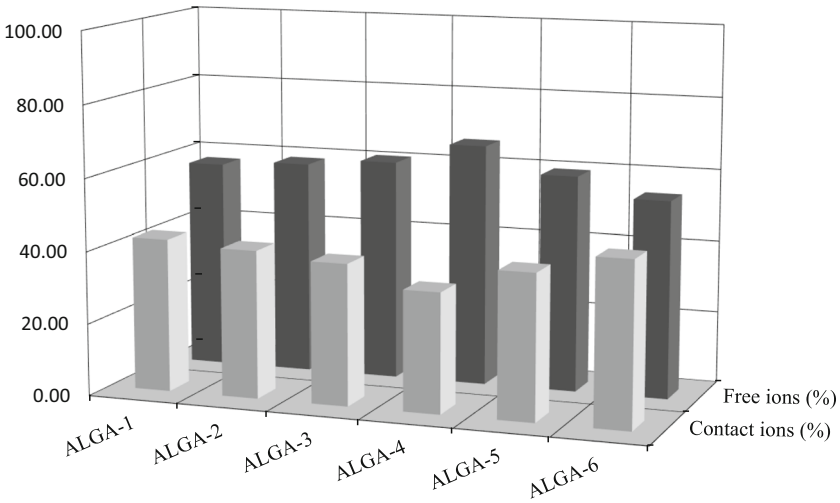

Fig. 11 Percentage of free and contact ions of the alginate-GA BBPEs system

Based on the percentage of free ions in Fig. 11, the number of ions mobility (μ), the number of density (η) and the diffusion coefficient number (D) were calculated using eq. (4), (5), (6) and (7) presented in Fig. 12.

Figure 12 depicts the ions mobility (μ) and the diffusion coefficient (D) show a similar trend with ionic conductivity where it rises sharply at ALGA-4 and dropped at ALGA-5. This behavior follows the trend of conductivity-composition of BBPEs system. The maximum ionic conductivity of alginate doped with GA (ALGA-4) exhibits maximum μ and D values of 2.14×10^{-9} cm^2 V^{-1} s^{-1} and 5.59×10^{-11} cm^2 s^{-1}, respectively. In the present work, the addition of GA in BBPEs system confirmed the conjecture in FTIR study where the H^+ from –OH jump to lone pair of $–COO^-$ from the polymer backbone. Moreover, the amorphousness structure and low glass transition, T_g of BBPEs system depict that ion easily to hop from one site to another with less activation energy needed. Besides, the diffusion ions, D of polymer matrix will contribute to the increment of ionic conductivity where the movement of the ions to the BBPEs system easily to interact [22].

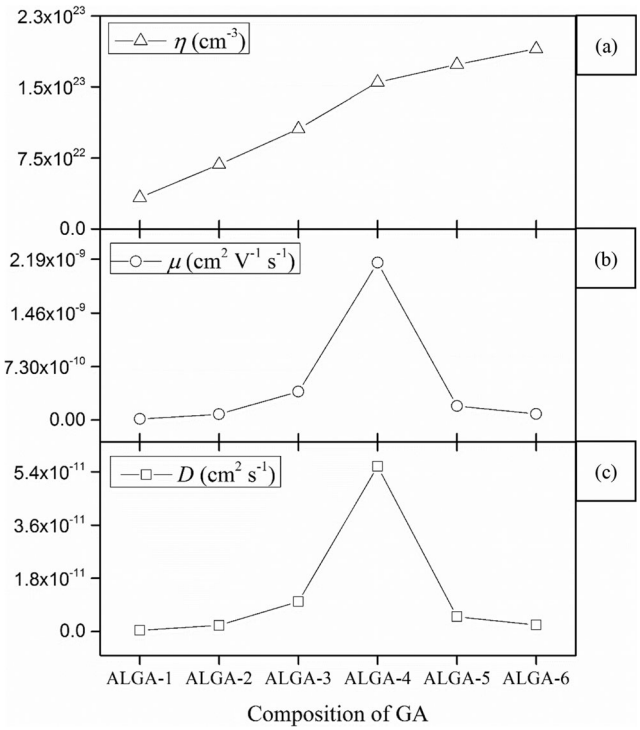

Fig. 12 The transport parameters for (**a**) number of mobile ions, η, (**b**) ions mobility, μ, and (**c**) diffusion coefficient, D of alginate-GA BBPEs system

It shows that the number density (η) of ions increased linearly with the composition of GA. The highest value of η is 1.90×10^{23} cm^{-3} were in contrast to the ionic conductivity due to the ALGA-6 higher than the optimum composition of GA at ALGA-4. The increment of η inferred that the GA in the polymer matrix was too heavy, contributed to the decreasing of ion mobility (μ) and diffusion coefficient (D), which affected by the formation of ion cluster and also overcrowding of mobile ions (H^+) [91]. In addition, increasing of crystallinity as shown from XRD analysis for higher composition of GA lead to overcrowding of ions since the re-crystalline phase tries to block any ion to migrate towards coordination site in polymer host [32]. With the addition beyond 20 wt. % of GA in BBPEs system, the increase in η lead to difficulty of ionic mobility to move, which in turn reduce the μ and D value.

Conclusion

The study on structural and transports properties of alginate doped with the different composition of GA as a potential proton-conducting bio-based polymer electrolytes (BBPEs) was carried out in the present work. The FTIR studies showed the presence of complexation between alginate and GA due to protonation which also called as Grotthuss mechanism where there is a strong contribution of hydrogen bonding related with

the coordination site of carboxylate ($–COO^-$) group of alginate. The ionic conductivity of alginate-GA system was found to increase from 8.74×10^{-8} S cm^{-1} to optimum value at 5.32×10^{-5} S cm^{-1} when was added with 20 wt. % of GA by showing an improvement of amorphous phase and thermal stability. Based on IR-deconvolution approach, it shows that the ionic conductivity of BBPEs was governed by ionic mobility (μ) and the diffusion coefficient number (D). The results suggest that the bio-based polymer electrolytes by using alginate materials have a good potential for applications as proton-conducting electrolytes system, which can be applied in electrochemical devices.

Acknowledgements The authors would like to thank Ministry of High Education (MOHE) for FRGS (FRGS/1/2019/STG07/UMP/02/4: RDU 1901114), Faculty of Industrial Science & Technology for the research support and Universiti Malaysia Pahang for providing Master Research Scheme (MRS).

References

1. Milczarek G, Inganäs O (2012) Renewable cathode materials from biopolymer/conjugated polymer interpenetrating networks. Science 335(6075):1468–1471. https://doi.org/10.1126/science.1215159
2. Singh R, Bhattacharya B, Tomar SK, Singh V, Singh PK (2017) Electrical, optical and electrophotochemical studies on agarose based biopolymer electrolyte towards dye sensitized solar cell application. Measurement 102:214–219. https://doi.org/10.1016/j.measurement.2017.02.014
3. Pawlicka A, Firmino A, Vieira D, Sentanin F, Grote JG, Kajzar F Gelatin-and DNA-based ionic conducting membranes for electrochromic devices. In: Optical Materials in Defence Systems Technology VI, 2009. International Society for Optics and Photonics, p 74870J. https://doi.org/10.1117/12.835913
4. Teoh KH, Lim C-S, Liew C-W, Ramesh S (2015) Electric double-layer capacitors with corn starch-based biopolymer electrolytes incorporating silica as filler. Ionics 21(7):2061–2068. https://doi.org/10.1007/s11581-014-1359-x
5. Karthikeyan S, Selvasekarapandian S, Premalatha M, Monisha S, Boopathi G, Aristatil G, Arun A, Madeswaran S (2017) Proton-conducting I-carrageenan-based biopolymer electrolyte for fuel cell application. Ionics 23(10):2775–2780. https://doi.org/10.1007/s11581-016-1901-0
6. Croisier F, Jérôme C (2013) Chitosan-based biomaterials for tissue engineering. Eur Polym J 49(4):780–792. https://doi.org/10.1016/j.eurpolymj.2012.12.009
7. Tan YM, Lim SH, Tay BY, Lee MW, Thian ES (2015) Functional chitosan-based grapefruit seed extract composite films for applications in food packaging technology. Mater Res Bull 69:142–146. https://doi.org/10.1016/j.materresbull.2014.11.041
8. Ahmad NH, Isa MIN Structural and ionic conductivity studies of CMC based polymerelectrolyte doped with NH_4Cl. In: Advanced Materials Research, 2015. Trans Tech Publ, pp 247–252. https://doi.org/10.4028/www.scientific.net/AMR.1107.247
9. Du JF, Bai Y, Pan DA, Chu WY, Qiao LJ (2009) Characteristics of proton conducting polymer electrolyte based on chitosan acetate complexed with CH_3COONH_4. J Polym Sci B Polym Phys 47(6):549–554. https://doi.org/10.1002/polb.21656
10. Khiar ASA, Arof AK (2010) Conductivity studies of starch-based polymer electrolytes. Ionics 16(2):123–129. https://doi.org/10.1007/s11581-009-0356-y
11. Ahmad AH Electrical analysis of cornstarch-based polymer electrolyte doped with NaCl. In: Solid state phenomena, 2017. Trans Tech Publ, pp 347–351. https://doi.org/10.4028/www.scientific.net/SSP.268.347
12. Mobarak NN, Ramli N, Ahmad A, Rahman MYA (2012) Chemical interaction and conductivity of carboxymethyl κ-carrageenan based green polymer electrolyte. Solid State Ionics 224:51–57. https://doi.org/10.1016/j.ssi.2012.07.010
13. Yang J-M, Wang N-C, Chiu H-C (2014) Preparation and characterization of poly (vinyl alcohol)/sodium alginate blended membrane for alkaline solid polymer electrolytes membrane. J Membr Sci 457:139–148. https://doi.org/10.1016/j.memsci.2014.01.034
14. Lacoste C, El Hage R, Bergeret A, Corn S, Lacroix P (2018) Sodium alginate adhesives as binders in wood fibers/textile waste fibers biocomposites for building insulation. Carbohydr Polym 184:1–8. https://doi.org/10.1016/j.carbpol.2017.12.019
15. Lu Y, Wang R, He J, Xu P, Li H, Tian L, Guo C (2019) Synthesis of bimetallic CoMn-alginate and synergistic effect on thermal decomposition of ammonium perchlorate. Mater Res Bull 117:1–8. https://doi.org/10.1016/j.materresbull.2019.04.013
16. Treenate P, Monvisade P, Yamaguchi M (2014) Development of hydroxyethylacryl chitosan/alginate hydrogel films for biomedical application. J Polym Res 21(12):601. https://doi.org/10.1007/s10965-014-0601-6
17. Yu C, Li X, Liu Z, Yang X, Huang Y, Lin J, Zhang J, Tang C (2016) Synthesis of hierarchically porous TiO_2 nanomaterials using alginate as soft templates. Mater Res Bull 83:609–614. https://doi.org/10.1016/j.materresbull.2016.07.014
18. Salama HE, Aziz MSA, Sabaa MW (2018) Novel biodegradable and antibacterial edible films based on alginate and chitosan biguanidine hydrochloride. Int J Biol Macromol 116:443–450. https://doi.org/10.1016/j.ijbiomac.2018.04.183
19. Aziz SB, Woo TJ, Kadir MFZ, Ahmed HM (2018) A conceptual review on polymer electrolytes and ion transport models. Journal of Science: Advanced Materials and Devices 3(1):1–17. https://doi.org/10.1016/j.jsamd.2018.01.002
20. Ngai KS, Ramesh S, Ramesh K, Juan JC (2016) A review of polymer electrolytes: fundamental, approaches and applications. Ionics 22(8):1259–1279. https://doi.org/10.1007/s11581-016-1756-4
21. Shukur MF, Kadir MFZ (2015) Electrical and transport properties of NH_4Br-doped cornstarch-based solid biopolymer electrolyte. Ionics 21(1):111–124. https://doi.org/10.1007/s11581-014-1157-5
22. Salleh NS, Aziz SB, Aspanut Z, Kadir MFZ (2016) Electrical impedance and conduction mechanism analysis of biopolymer electrolytes based on methyl cellulose doped with ammonium iodide. Ionics 22(11):2157–2167. https://doi.org/10.1007/s11581-016-1731-0
23. Monisha S, Mathavan T, Selvasekarapandian S, Benial AMF (2017) Preparation and characterization of cellulose acetate and lithium nitrate for advanced electrochemical devices. Ionics 23(10):2697–2706. https://doi.org/10.1007/s11581-016-1886-8
24. Kumar LS, Selvin PC, Selvasekarapandian S, Manjuladevi R, Monisha S, Perumal P (2018) Tamarind seed polysaccharide biopolymer membrane for lithium-ion conducting battery. Ionics:1–11. https://doi.org/10.1007/s11581-018-2541-3
25. Sudhakar YN, Selvakumar M, Bhat DK (2015) Preparation and characterization of phosphoric acid-doped hydroxyethyl cellulose electrolyte for use in supercapacitor. Materials for Renewable and Sustainable Energy 4(3):10. https://doi.org/10.1007/s40243-015-0051-z
26. Fadzallah IA, Majid SR, Careem MA, Arof AK (2014) A study on ionic interactions in chitosan–oxalic acid polymer electrolyte

membranes. J Membr Sci 463:65–72. https://doi.org/10.1016/j.memsci.2014.03.044
27. Senthilkumar P, Ganesh T, Vinoth K, Maria Sylvester M, Anand Karunakaran DJS, Hudge P, Kumbharakhane AC (2019) Dielectric relaxation and molecular interaction investigation of glycolic acid-water mixture using time domain reflectometry. Indian Journal of Pure & Applied Physics (IJPAP) 57(3):180–187
28. Bakhshi A, Bhalla G (2004) Electrically conducting polymers: materials of the twentyfirst century
29. Samsudin AS, Isa MIN (2012) Structural and electrical properties of carboxy methylcellulose-dodecyltrimethyl ammonium bromide-based biopolymer electrolytes system. Int J Polymer Mater 61(1): 30–40. https://doi.org/10.1080/00914037.2011.557810
30. Dey A, Karan S, Dey A, De SK (2011) Structure, morphology and ionic conductivity of solid polymer electrolyte. Mater Res Bull 46(11):2009–2015. https://doi.org/10.1016/j.materresbull.2011.07.008
31. Ranjana PAB, Jeya S, Abarna S, Premalatha M, Arulsankar A, Sundaresan B (2019) Enhancement of Na+ ion conduction in polymer blend electrolyte P (VdF-HFP)–PMMA-NaTf by the inclusion of EC. J Polym Res 26(2):38. https://doi.org/10.1007/s10965-019-1704-x
32. Zainuddin NK, Samsudin AS (2018) Investigation on the effect of NH_4Br at transport properties in K–carrageenan based biopolymer electrolytes via structural and electrical analysis. Mater Today Comm 14:199–209. https://doi.org/10.1016/j.mtcomm.2018.01.004
33. Rasali NMJ, Samsudin AS (2017) Ionic transport properties of protonic conducting solid biopolymer electrolytes based on enhanced carboxymethyl cellulose-NH_4Br with glycerol. Ionics:1–12. https://doi.org/10.1007/s11581-017-2318-0
34. Aprilliza M. Characterization and properties of sodium alginate from brown algae used as an ecofriendly superabsorbent. In: IOP Conference Series: Materials Science and Engineering, 2017. vol 1. IOP Publishing, p 012019. https://doi.org/10.1088/1757-899X/188/1/012019
35. Hu Y, Zhang S, Han D, Ding Z, Zeng S, Xiao X (2018) Construction and evaluation of the hydroxypropyl methyl cellulose-sodium alginate composite hydrogel system for sustained drug release. J Polym Res 25(7):148. https://doi.org/10.1007/s10965-018-1546-y
36. Fawzy MA, Gomaa M, Hifney AF, Abdel-Gawad KM (2017) Optimization of alginate alkaline extraction technology from Sargassum latifolium and its potential antioxidant and emulsifying properties. Carbohydr Polym 157:1903–1912. https://doi.org/10.1016/j.carbpol.2016.11.077
37. Bardajee GR, Hooshyar Z, Soleyman R (2017) Nanocomposites of sodium alginate biopolymer and CdTe/ZnS quantum dots for fluorescent determination of amantadine. J Polym Res 24(8):128. https://doi.org/10.1007/s10965-017-1247-y
38. Botvin V, Latypov A, Ponarin N, Filimoshkin A. Synthesis of glycolide by catalytic depolymerization of glycolic acid oligomers modified by polyhydric alcohols. In: Journal of Physics: Conference Series, 2019. vol 1. IOP Publishing, p 012019. https://doi.org/10.1088/1742-6596/1145/1/012019,
39. Varghese HT, Panicker CY (2011) IR, Raman and Ab-initio Calcualtions of glycolic acid. Orient J Chem 27(1):215–220
40. Ramlli MA, Bashirah NAA, Isa MIN Ionic Conductivity and Structural Analysis of 2-hyroxyethyl Cellulose Doped with Glycolic Acid Solid Biopolymer Electrolytes for Solid Proton Battery. In: IOP Conference Series: Materials Science and Engineering (2018) vol 1. IOP Publishing, p 012038. https://doi.org/10.1088/1757-899X/440/1/012038
41. Hay MB, Myneni SCB (2007) Structural environments of carboxyl groups in natural organic molecules from terrestrial systems. Part 1: infrared spectroscopy. Geochim Cosmochim Acta 71(14):3518–3532. https://doi.org/10.1016/j.gca.2007.03.038
42. Ahokas JM, Kosendiak I, Krupa J, Wierzejewska M, Lundell J (2019) Raman spectroscopy of glycolic acid complexes with N2. J Mol Struct 1183:367–372. https://doi.org/10.1016/j.molstruc.2019.01.080
43. Sikkanthar S, Karthikeyan S, Selvasekarapandian S, Pandi DV, Nithya S, Sanjeeviraja C (2015) Electrical conductivity characterization of polyacrylonitrile-ammonium bromide polymer electrolyte system. J Solid State Electrochem 19(4):987–999. https://doi.org/10.1007/s10008-014-2697-3
44. Lopes S, Bueno L, AGUIAR JÚNIOR FD, Finkler C (2017) Preparation and characterization of alginate and gelatin microcapsules containing lactobacillus rhamnosus. Anais da academia Brasileira de Ciências (AHEAD):0-0. https://doi.org/10.1590/0001-3765201720170071
45. Ramlli MA, Isa MIN (2016) Structural and ionic transport properties of protonic conducting solid biopolymer electrolytes based on Carboxymethyl cellulose doped with ammonium fluoride. J Phys Chem B 120(44):11567–11573. https://doi.org/10.1021/acs.jpcb.6b06068
46. Huang X, Zheng Q, Fang X, Shao H (2018) Probing qualitative change in intermolecular forces from hydrogen bonding to electrostatic interaction on the surface of self-assembled monolayer. J Electrochem Soc 165(5):H240–H246. https://doi.org/10.1149/2.0731805jes
47. Bakhtin S, Shved E, Bespal'ko Y (2017) Nucleophile-electrophile interactions in the reaction of oxiranes with carboxylic acids in the presence of tertiary amines. J Phys Org Chem 30(12). https://doi.org/10.1002/poc.3717
48. Monisha S, Mathavan T, Selvasekarapandian S, Benial AMF, Aristatil G, Mani N, Premalatha M (2017) Investigation of bio polymer electrolyte based on cellulose acetate-ammonium nitrate for potential use in electrochemical devices. Carbohydr Polym 157: 38–47. https://doi.org/10.1016/j.carbpol.2016.09.026
49. Samsudin AS, Khairul WM, Isa MIN (2012) Characterization on the potential of carboxy methylcellulose for application as proton conducting biopolymer electrolytes. J Non-Cryst Solids 358(8): 1104–1112. https://doi.org/10.1016/j.jnoncrysol.2012.02.004
50. Samsudin AS, Lai HM, Isa MIN (2014) Biopolymer materials based carboxymethyl cellulose as a proton conducting biopolymer electrolyte for application in rechargeable proton battery. Electrochim Acta 129:1–13. https://doi.org/10.1016/j.electacta.2014.02.074
51. Chai MN, Isa MIN (2013) The oleic acid composition effect on the carboxymethyl cellulose based biopolymer electrolyte. Journal of Crystallization Process and Technology 3(01):1–4. https://doi.org/10.4236/jcpt.2013.31001
52. Alakanandana A, Subrahmanyam AR, Kumar JS (2016) Structural and electrical conductivity studies of pure PVA and PVA doped with succinic acid polymer electrolyte system. Mater, Today: Proceedings 3(10):3680–3688. https://doi.org/10.1016/j.matpr.2016.11.013
53. Rikukawa M, Sanui K (2000) Proton-conducting polymer electrolyte membranes based on hydrocarbon polymers. Prog Polym Sci 25(10):1463–1502. https://doi.org/10.1016/S0079-6700(00)00032-0
54. Liew C-W, Ramesh S (2013) Studies on ionic liquid-based corn starch biopolymer electrolytes coupling with high ionic transport number. Cellul 20(6):3227–3237. https://doi.org/10.1007/s10570-013-0079-0
55. Qu X, Wirsen A, Albertsson A-C (2000) Effect of lactic/glycolic acid side chains on the thermal degradation kinetics of chitosan derivatives. Polym 41(13):4841–4847. https://doi.org/10.1016/S0032-3861(99)00704-1

56. Rani MSA, Rudhziah S, Ahmad A, Mohamed NS (2014) Biopolymer electrolyte based on derivatives of cellulose from kenaf bast fiber. Polym 6(9):2371–2385. https://doi.org/10.3390/polym6092371
57. Saadiah MA, Zhang D, Nagao Y, Muzakir SK, Samsudin AS (2019) Reducing crystallinity on thin film based CMC/PVA hybrid polymer for application as a host in polymer electrolytes. J Non-Cryst Solids 511:201–211. https://doi.org/10.1016/j.jnoncrysol.2018.11.032
58. Shukur MF, Ithnin R, Kadir MFZ (2014) Electrical properties of proton conducting solid biopolymer electrolytes based on starch–chitosan blend. Ionics 20(7):977–999. https://doi.org/10.1007/s11581-013-1033-8
59. Mazuki NF, Fuzlin AF, Saadiah MA, Samsudin AS (2018) An investigation on the abnormal trend of the conductivity properties of CMC/PVA-doped NH_4Cl-based solid biopolymer electrolyte system. Ionics:1–11. https://doi.org/10.1007/s11581-018-2734-9
60. Samsudin AS, Saadiah MA (2018) Ionic conduction study of enhanced amorphous solid bio-polymer electrolytes based carboxymethyl cellulose doped NH_4Br. J Non-Cryst Solids 497:19–29. https://doi.org/10.1016/j.jnoncrysol.2018.05.027
61. Chitra R, Sathya P, Selvasekarapandian S, Monisha S, Moniha V, Meyvel S (2018) Synthesis and characterization of iota-carrageenan solid biopolymer electrolytes for electrochemical applications. Ionics 25:1–11. https://doi.org/10.1007/s11581-018-2687-z
62. Li X, Xie H, Lin J, Xie W, Ma X (2009) Characterization and biodegradation of chitosan–alginate polyelectrolyte complexes. Polym Degrad Stab 94(1):1–6. https://doi.org/10.1016/j.polymdegradstab.2008.10.017
63. Perumal P, Selvin PC, Selvasekarapandian S (2018) Characterization of biopolymer pectin with lithium chloride and its applications to electrochemical devices. Ionics 24(10):3259–3270. https://doi.org/10.1007/s11581-018-2507-5
64. Ghosal K, Das A, Das SK, Mahmood S, Ramadan MAM, Thomas S (2019) Synthesis and characterization of interpenetrating polymeric networks based bio-composite alginate film: a well-designed drug delivery platform. Int J Biol Macromol 130:645–654. https://doi.org/10.1016/j.ijbiomac.2019.02.117
65. Rezvanian M, Ahmad N, Amin MCIM, Ng S-F (2017) Optimization, characterization, and in vitro assessment of alginate-pectin ionic cross-linked hydrogel film for wound dressing applications. Int J Biol Macromol 97:131–140. https://doi.org/10.1016/j.ijbiomac.2016.12.079
66. Sampathkumar L, Selvin PC, Selvasekarapandian S, Perumal P, Chitra R, Muthukrishnan M (2019) Synthesis and characterization of biopolymer electrolyte based on tamarind seed polysaccharide, lithium perchlorate and ethylene carbonate for electrochemical applications. Ionics 25(3):1067–1082. https://doi.org/10.1007/s11581-019-02857-1
67. Rasali NMJ, Nagao Y, Samsudin AS (2018) Enhancement on amorphous phase in solid biopolymer electrolyte based alginate doped NH_4NO_3. Ionics:1–14. https://doi.org/10.1007/s11581-018-2667-3
68. Kadir MFZ, Hamsan MH (2018) Green electrolytes based on dextran-chitosan blend and the effect of NH_4SCN as proton provider on the electrical response studies. Ionics 24(8):2379–2398. https://doi.org/10.1007/s11581-017-2380-7
69. Moniha V, Alagar M, Selvasekarapandian S, Sundaresan B, Boopathi G (2018) Conductive bio-polymer electrolyte iota-carrageenan with ammonium nitrate for application in electrochemical devices. J Non-Cryst Solids 481:424–434. https://doi.org/10.1016/j.jnoncrysol.2017.11.027
70. Gao C, Pollet E, Avérous L (2017) Properties of glycerol-plasticized alginate films obtained by thermo-mechanical mixing. Food Hydrocoll 63:414–420. https://doi.org/10.1016/j.foodhyd.2016.09.023
71. Larosa C, Salerno M, de Lima JS, Meri RM, da Silva MF, de Carvalho LB, Converti A (2018) Characterisation of bare and tannase-loaded calcium alginate beads by microscopic, thermogravimetric, FTIR and XRD analyses. Int J Biol Macromol 115:900–906. https://doi.org/10.1016/j.ijbiomac.2018.04.138
72. Choe SR, Haldorai Y, Jang S-C, Rethinasabapathy M, Lee Y-C, Han Y-K, Jun Y-S, Roh C, Huh YS (2018) Fabrication of alginate/humic acid/Fe-aminoclay hydrogel composed of a grafted-network for the efficient removal of strontium ions from aqueous solution. Environ Technol Innov 9:285–293. https://doi.org/10.1016/j.eti.2017.12.008
73. Yusof YM, Illias HA, Kadir MFZ (2014) Incorporation of NH_4Br in PVA-chitosan blend-based polymer electrolyte and its effect on the conductivity and other electrical properties. Ionics 20(9):1235–1245. https://doi.org/10.1007/s11581-014-1096-1
74. Samsudin AS, Isa MIN (2012) Structural and ionic transport study on CMC doped NH_4Br: a new types of biopolymer electrolytes. J Appl Sci 12(2):174–179. https://doi.org/10.3923/jas.2012.174.179
75. Kadir MFZ, Salleh NS, Hamsan MH, Aspanut Z, Majid NA, Shukur MF (2018) Biopolymeric electrolyte based on glycerolized methyl cellulose with NH_4Br as proton source and potential application in EDLC. Ionics 24(6):1651–1662. https://doi.org/10.1007/s11581-017-2330-4
76. Karthikeyan S, Sikkanthar S, Selvasekarapandian S, Arunkumar D, Nithya H, Kawamura J (2016) Structural, electrical and electrochemical properties of polyacrylonitrile-ammonium hexaflurophosphate polymer electrolyte system. J Polym Res 23(3):51. https://doi.org/10.1007/s10965-016-0952-2
77. Shukur MF, Ibrahim FM, Majid NA, Ithnin R, Kadir MFZ (2013) Electrical analysis of amorphous corn starch-based polymer electrolyte membranes doped with LiI. Phys Scr 88(2):025601. https://doi.org/10.1088/0031-8949/88/02/025601
78. Kadir MFZ, Majid SR, Arof AK (2010) Plasticized chitosan–PVA blend polymer electrolyte based proton battery. Electrochim Acta 55(4):1475–1482. https://doi.org/10.1016/j.electacta.2009.05.011
79. Aziz NAN, Idris NK, Isa MIN (2010) Proton conducting polymer electrolytes of methylcellulose doped ammonium fluoride: conductivity and ionic transport studies. Int J Phy Sci 5(6):748–752. https://doi.org/10.5897/IJPS
80. Fuzlin AF, Rasali NMJ, Samsudin AS. Effect on ammonium bromide in dielectric behavior based alginate solid biopolymer electrolytes. In: IOP Conference Series: Materials Science and Engineering, 2018. vol 1. IOP Publishing, p 012080. https://doi.org/10.1088/1757-899X/342/1/012080
81. Tripathy T, Kolya H, Jana S (2018) Selective lead (II) adsorption and flocculation characteristics of the grafted sodium alginate: a comparative study. J Polym Environ 26(3):926–937. https://doi.org/10.1007/s10924-017-1004-7
82. Othman L, Isa KBM, Osman Z, Yahya R (2017) Ionic transport studies of gel polymer electrolytes containing sodium salt. Mater, Today: Proceedings 4(4):5122–5129. https://doi.org/10.1016/j.matpr.2017.05.017
83. Premalatha M, Mathavan T, Selvasekarapandian S, Selvalakshmi S, Monisha S (2017) Incorporation of NH_4Br in tamarind seed polysaccharide biopolymer and its potential use in electrochemical energy storage devices. Org Electron 50:418–425. https://doi.org/10.1016/j.orgel.2017.08.017
84. Mohan VM, Qiu W, Shen J, Chen W (2010) Electrical properties of poly (vinyl alcohol)(PVA) based on LiFePO 4 complex polymer electrolyte films. J Polym Res 17(1):143–150. https://doi.org/10.1007/s10965-009-9300-0
85. Kim D-S, Woo JC, Youk JH, Manuel J, Ahn J-H (2014) Gel polymer electrolytes based on nanofibrous polyacrylonitrile–acrylate for lithium batteries. Mater Res Bull 58:208–212. https://doi.org/10.1016/j.materresbull.2014.01.047

86. Sinha R, Basu S, Meikap AK (2018) The investigation of the electrical transport properties of Gd doped $YCrO_3$ nanoparticles. Mater Res Bull 97:578–587. https://doi.org/10.1016/j.materresbull.2017.08.055
87. Sohaimy MIH, Isa MIN (2017) Ionic conductivity and conduction mechanism studies on cellulose based solid polymer electrolytes doped with ammonium carbonate. Polym Bull 74(4):1371–1386. https://doi.org/10.1007/s00289-016-1781-5
88. Kopitzke RW, Linkous CA, Anderson HR, Nelson GL (2000) Conductivity and water uptake of aromatic-based proton exchange membrane electrolytes. J Electrochem Soc 147(5):1677–1681. https://doi.org/10.1149/1.1393417
89. Fuzlin AF, Nagao Y, Misnon II, Samsudin AS (2019) Studies on structural and ionic transport in biopolymer electrolytes based on alginate-LiBr. Ionics:1–16. https://doi.org/10.1007/s11581-019-03386-7
90. Chai MN, Isa MIN (2016) Novel proton conducting solid biopolymer electrolytes based on carboxymethyl cellulose doped with oleic acid and plasticized with glycerol. Sci Rep 6:27328. https://doi.org/10.1038/srep27328
91. Sohaimy MIH, Isa MIN (2015) Effect of ammonium carbonate salt concentration on structural and ionic conductivity of cellulose based solid polymer electrolytes. Fibers Polym 16(5):1031–1034. https://doi.org/10.1007/s12221-015-1031-8